VOL. 8, NO. 5, MAY 2013 ISSN 1819-6608
ARPN Journal of Engineering and Applied Sciences

www.arpnjournals.com

NUMERICAL SIMULATION OF NOZZLE FLOW WITH CHEMICAL EQUILIBRIUM

Mohamed A. Al Kady and Farouk M. Owis
Aerospace Engineering Department, Faculty of Engineering, Cairo University Cairo, Egypt
E-Mail: fowis@eng.cu.edu.eg

ABSTRACT

The compressible two-dimensional planar and axisymmetric Navier-Stokes equations are solved in generalized curvilinear coordinates to simulate non-reacting and chemical equilibrium nozzle flows. A zonal turbulence model of $k-\omega$ is used in the simulations to compute the eddy viscosity. A numerical method is developed to discretize the governing equations using the finite difference technique. The convective terms in the governing equations are solved numerically using a second order flux difference splitting method of Roe while a second order central difference is used for the viscous terms. The discretized equations are integrated implicitly in time to increase the stability of the numerical scheme. The flow solver is coupled with a chemical equilibrium module to compute the composition of gas mixture of known enthalpy and pressure. Few test cases are performed to illustrate the capabilities of the flow solver to predict nozzle flow with and without chemical equilibrium. The results are compared with the published data and the results are in good agreement with those published simulations of the same test cases.

Keywords: nozzle flow, chemical equilibrium, turbulent flow, upwind schemes, roe scheme.

Nomenclature

C	Speed of sound
D_{th}	Throat diameter
h	Enthalpy
p	Pressure
P_r	Prandtle number
P_{rt}	Turbulent Prandtle number
Ru	Universal gas constant
Re	Reynolds number
t	Physical time
T	Temperature
u	Velocity in x_1-direction
v	Velocity in x_2-direction
μ	Fluid viscosity
μ_t	Turbulent eddy viscosity
ϕ	Dissipation term
φ	Equivalence ratio
φ_s	Stoichiomertric mixture ratio
ρ	Fluid density

1. INTRODUCTION

In recent years, there has been a renewed interest in hypersonic gas dynamics and supersonic turbulent reacting flows. In this context, flow problems involving chemical activity of fuel and oxidizer mixtures have received widespread attention. Finite rate chemistry calculations have been successfully attempted by several investigators such as Cinnella [1].

The actual expansion process in a rocket or ramjet nozzle is intermediate between the extremes of frozen and equilibrium flow, with the latter producing higher performance due to recovery of some of the chemical energy tied up in the decomposition of complex molecular species in the chamber. Flow simulations performed using the assumption of the chemical equilibrium assumption have the potential of yielding results at a fraction of the computational cost associated with an equivalent finite rate calculation. A flow solver based on chemical equilibrium requires solving only the four basic flow equations in two dimensions instead of N+3 that are necessary for a finite rate solver, where N is the number of chemical species. Moreover, the equilibrium composition of a mixture of gases is well known from classical thermodynamics, and the thermodynamic data for gaseous species are will established. Unfortunately, chemical equilibrium is only a limiting case of real life finite rate chemistry, with the limit taken for reactions rates going to infinity, and the accuracy of its predictions should be investigated for each class of problems of interest. Nevertheless, the aforementioned numerical and physical difficulties associated with finite rate simulations render chemical equilibrium a very attractive tool for the scientist and engineer, in particular when the driving consideration is a relative inexpensive inclusion of real gas effects.

Numerical simulation of high-speed, compressible, turbulent and reacting coaxial jet flow is performed by Mehta [2]. Numerical analysis has been performed using a cell-centered finite volume discretization in conjunction with three-stage Rung-Kutta time stepping scheme. Turbulence is described by a $k-\varepsilon$ two equations model. The eddy break-up model is applied for turbulent diffusion flames. A considerable amount of computational time is saved in the evaluation of the viscous flux vectors using a simple structured grid arrangement. The numerical algorithm has been tested for the well-documented supersonic burner problem.

Westmoreland and Cinnella [3] focused their work on the development of robust and efficient numerical techniques for the calculation of equilibrium composition and thermodynamic properties of mixtures of thermally

perfect gases. The approach chosen lends itself to the utilization as a Black-Box for the simulation of reacting flows of interest to the applied aerodynamics. The flow solver interacts with the chemical equilibrium solver through the exchange of inputs, such as density, internal energy, and initial guesses for temperature and composition, and output, such as speed of sound, isentropic index, pressure, and transport coefficients.

The objective of the current study is to develop a numerical tool that can be used to simulate fluid flows in rocket engines with the assumption of chemical equilibrium. The unsteady, turbulent and compressible Navier-Stokes equations are coupled with a set of chemical equilibrium equations to estimate the flow variables and the concentration of the products of combustion. The chemical reactions are assumed to be in chemical equilibrium at every grid point in the computational domain. The fluid flow equations are discretized on a structured grid using the finite difference method. The convection term is discretized using upwind differencing scheme that has uniformly high accuracy throughout the interior grid points. The viscous fluxes are differenced using second-order accurate central differences. A two-equation $k-\omega$ model is used for the turbulence closure. The model is a modified version of the model used by Rogers [4] to compute single-phase compressible flows. This model has different coefficients, depending on the region of solution, to reduce the free stream dependency of the model. The model switches from the $k-\omega$ model near the wall to the $k-\varepsilon$ model away from the wall. The variation of the mixture density is implemented in the current model as explained by Owis [5]. Finally, the results of the non-reactive and reactive flows are compared with published test cases.

2. GOVERNING EQUATIONS

The unsteady, compressible two-dimensional Navier-Stokes equations are used in the simulations. The governing equations for axisymmetric and planar flows are written in the following form:

$$\Gamma_e \frac{\partial Q}{\partial t}+\frac{\partial (E-E_v)}{\partial x}+\frac{\partial (F-F_v)}{\partial y}+\alpha (H-H_v)=0 \quad (1)$$

Where

$$F=\begin{bmatrix} \rho v \\ \rho u v \\ \rho v^2+\mathrm{p} \\ \rho \mathrm{h_t} v \end{bmatrix} \quad E=\begin{bmatrix} \rho u \\ \rho u^2+\mathrm{p} \\ \rho \mathrm{u\,v} \\ \rho \mathrm{h_t}\, u \end{bmatrix} \quad Q=\begin{bmatrix} \mathrm{p} \\ u \\ v \\ h \end{bmatrix}$$

$$\Gamma_e=\begin{bmatrix} \frac{\partial \rho}{\partial \mathrm{P}} & 0 & 0 & \frac{\partial \rho}{\partial \mathrm{h}} \\ \mathrm{u}\frac{\partial \rho}{\partial \mathrm{P}} & \rho & 0 & u\frac{\partial \rho}{\partial \mathrm{h}} \\ \mathrm{v}\frac{\partial \rho}{\partial \mathrm{P}} & 0 & \rho & v\frac{\partial \rho}{\partial \mathrm{h}} \\ \mathrm{h_t}\frac{\partial \rho}{\partial \mathrm{P}}-1 & u\rho & v\rho & ht\frac{\partial \rho}{\partial \mathrm{h}}+\rho \end{bmatrix} \quad H=\frac{1}{y}\begin{bmatrix} \rho v \\ \rho u v \\ \rho v^2 \\ \rho h_t v \end{bmatrix}$$

$$F_v=\begin{bmatrix} 0 \\ \tau_{xy} \\ \tau_{yy} \\ u\tau_{xy}+v\tau_{yy}-q_y \end{bmatrix} \quad E_v=\begin{bmatrix} 0 \\ \tau_{xx} \\ \tau_{xy} \\ u\tau_{xx}+v\tau_{xy}-q_x \end{bmatrix}$$

$$H_v=\frac{1}{y}\begin{bmatrix} 0 \\ \tau_{xy}-\frac{2}{3}\frac{y}{R_e}\frac{\partial}{\partial x}(\mu\frac{v}{y}) \\ \tau_{yy}-\tau_{\theta\theta}-\frac{2}{3}\frac{\mu}{y}v-\frac{2}{3}\frac{y}{R_e}\frac{\partial}{\partial y}(\mu\frac{v}{y}) \\ u\tau_{xy}+v\tau_{yy}-q_y-\frac{2}{3}\frac{\mu}{R_e}(\frac{v^2}{y})-\frac{y}{R_e}\frac{\partial}{\partial y}(\frac{2}{3}\mu\frac{v^2}{y})-\frac{y}{R_e}\frac{\partial}{\partial x}(\frac{2}{3}\mu\frac{uv}{y}) \end{bmatrix}$$

Where Q is the solution vector, E and F are called the flux vectors, and H is the source term.

α =1 for axisymmetric flow
α =0 for planar flow

u is the velocity component in axial direction, v is the velocity component in radial direction, p is the pressure, *h* is the enthalpy, ρ is the density, and h_t is the total enthalpy. Where the shear stresses τ and the heat flux q can be expressed as follows:

$$\tau_{xx}=\frac{2}{3}(\frac{\mu+\mu_t}{R_e})(2\frac{\partial \mathrm{u}}{\partial \mathrm{x}}-\frac{\partial \mathrm{v}}{\partial \mathrm{y}}) \quad \tau_{yy}=\frac{2}{3}(\frac{\mu+\mu_t}{R_e})(2\frac{\partial \mathrm{v}}{\partial \mathrm{y}}-\frac{\partial \mathrm{u}}{\partial \mathrm{x}})$$

$$\tau_{xy}=(\frac{\mu+\mu_t}{R_e})(\frac{\partial \mathrm{v}}{\partial \mathrm{x}}+\frac{\partial \mathrm{u}}{\partial \mathrm{y}}) \quad \tau_{\theta\theta}=(\frac{\mu+\mu_t}{R_e})(\frac{-2}{3}(\frac{\partial \mathrm{v}}{\partial \mathrm{y}}+\frac{\partial \mathrm{u}}{\partial \mathrm{x}})+\frac{4}{3}\frac{\mathrm{v}}{\mathrm{y}})$$

$$q_x=-(\frac{\mu}{\mathrm{p_r R_e}}+\frac{\mu_t}{\mathrm{p_{r_t} R_e}})\frac{\partial \mathrm{h}}{\partial \mathrm{x}} \quad q_y=-(\frac{\mu}{\mathrm{p_r R_e}}+\frac{\mu_t}{\mathrm{p_{r_t} R_e}})\frac{\partial \mathrm{h}}{\partial \mathrm{y}}$$

The governing equations can be rewritten in the generalized curvilinear coordinates as follows:

$$\Gamma_e \frac{\partial \overline{Q}}{\partial t}+\frac{\partial (\overline{E}-\overline{E_v})}{\partial \xi}+\frac{\partial (\overline{F}-\overline{F}_v)}{\partial \eta}+\alpha (\overline{H}-\overline{H}_v)=0 \quad (2)$$

Where

$$\overline{Q}=\frac{Q}{J}=\frac{1}{J}(p,u,v,h)^t$$

$$\overline{E} = \frac{1}{J}(\rho U, \rho uU + \mathrm{p}\xi_x, \rho vU + \mathrm{p}\xi_y, \rho h_t U)^t$$

$$\overline{F} = \frac{1}{J}(\rho V, \rho uV + \mathrm{p}\eta_x, \rho vV + \mathrm{p}\eta_y, \rho h_t V)^t$$

$$U = \xi_x u + \xi_y v, \quad \overline{H} = \frac{H}{J}$$
$$V = \eta_x u + \eta_y v$$

Where $\overline{E}_v, \overline{F}_v$ and $\overline{H}_v$ are the viscous fluxes in the generalized curvilinear coordinates.

3. TURBULENCE MODELING

A two-equation $k-\omega$ model is used for the turbulence closure. The model is a modified version of the model used by Rogers [4] to compute single-phase incompressible flows. This model has different coefficients, depending on the region of solution, to reduce the free stream dependency of the model. The model switches from the $k-\omega$ model near the wall to the $k-\varepsilon$ model away from the wall. The variation of the mixture density is implemented in the current model. The model is defined as follows:

$$\frac{\partial(\rho k)}{\partial t} + \frac{\partial}{\partial x_j}(\rho u_j k - (\mu + \sigma_k \mu_t)\frac{\partial \rho k}{\partial x_j}) = p_k - \beta^* \rho \omega k \quad (3)$$

$$\frac{\partial(\rho\omega)}{\partial t} + \frac{\partial}{\partial x_j}(\rho u_j \omega - (\mu + \sigma_\omega \mu_t)\frac{\partial \omega}{\partial x_j}) = \gamma p_w - \beta \rho \omega^2 + 2(1-F_1)\sigma_{\omega 2}\frac{\rho}{\omega}\frac{\partial k}{\partial x_j}\frac{\partial \omega}{\partial x_j} \quad (4)$$

$$P_k = \mu_t \Omega^2 \quad P_\omega = \Omega^2$$

Where p_k and p_ω are the production terms and Ω is the magnitude of the vorticity.

4. NUMERICAL SCHEME

Upwind difference schemes are used to compute the convective flux derivatives. The flux difference splitting of Roe [6] scheme is used to discretize the convective terms. In order to use the upwind flux differencing schemes, the Jacobian matrices of the flux vectors are required in addition to their eigensystem. The convective flux is linearized as explained by Owis [5],

$$\Gamma_e \frac{\partial \overline{Q}}{\partial t} + \Gamma_e \overline{A}\frac{\partial \overline{Q}}{\partial \xi} + \Gamma_e \overline{B}\frac{\partial \overline{Q}}{\partial \eta} + \alpha(\overline{H} - \overline{H}_v) = 0$$

Where $\overline{A} = \Gamma_e^{-1} A,\ \overline{B} = \Gamma_e^{-1} B,\quad A = \frac{\partial \overline{E}}{\partial \overline{Q}},\ B = \frac{\partial \overline{F}}{\partial \overline{Q}}$

$$A = \begin{bmatrix} \frac{\partial \rho}{\partial p}U & \rho\xi_x & \rho\xi_y & \frac{\partial \rho}{\partial h}U \\ \xi_x + \frac{\partial \rho}{\partial p}uU & \rho(U + u\xi_x) & \rho\xi_y u & \frac{\partial \rho}{\partial h}uU \\ \xi_y + \frac{\partial \rho}{\partial p}vU & \rho\xi_x v & \rho(\xi_y v + U) & \frac{\partial \rho}{\partial h}vU \\ \frac{\partial \rho}{\partial p}h_t U & \rho(\xi_x h_t + uU) & \rho(\xi_y h_t + vU) & \rho U + \frac{\partial \rho}{\partial h}Uh_t \end{bmatrix}$$

$$\overline{A} = \begin{bmatrix} U & \frac{\xi_x \rho^2}{\frac{\partial \rho}{\partial h} + \rho\frac{\partial \rho}{\partial p}} & \frac{\xi_y \rho^2}{\frac{\partial \rho}{\partial h} + \rho\frac{\partial \rho}{\partial p}} & 0 \\ \frac{\xi_x}{\rho} & U & 0 & 0 \\ \frac{\xi_y}{\rho} & 0 & U & 0 \\ 0 & \frac{\xi_x \rho^2}{\frac{\partial \rho}{\partial h} + \rho\frac{\partial \rho}{\partial p}} & \frac{\xi_y \rho^2}{\frac{\partial \rho}{\partial h} + \rho\frac{\partial \rho}{\partial p}} & U \end{bmatrix}$$

$$\lambda = \{U, U, U - \overline{c}, U + \overline{c}\}$$

Where λ is the eigenvalues of the matrix $\overline{A}$

$$\overline{c} = c\sqrt{\xi_x^2 + \xi_y^2}$$

Where c is the speed of sound for compressible flow, which can be expressed as:

$$\frac{1}{c^2} = \frac{\partial \rho}{\partial p} + \frac{1}{\rho}\frac{\partial \rho}{\partial h}$$

The right eigenvector and the inverse of the right eigenvector matrices are given by:

$$X_i = \begin{bmatrix} 0 & 0 & \rho\overline{c} & 0 \\ -\xi_y & -\xi_x & -\xi_x & 0 \\ \xi_x & -\xi_y & -\xi_y & 0 \\ 0 & 0 & \overline{c} & 1 \end{bmatrix}$$

$$X_i^{-1} = \begin{bmatrix} 0 & -\frac{\xi_y}{\xi_x^2 + \xi_y^2} & \frac{\xi_x}{(\xi_x^2 + \xi_y^2)} & 0 \\ -\frac{1}{\rho\overline{c}} & -\frac{\xi_x}{(\xi_x^2 + \xi_y^2)} & -\frac{\xi_y}{(\xi_x^2 + \xi_y^2)} & 0 \\ -\frac{1}{\rho\overline{c}} & 0 & 0 & 0 \\ \frac{1}{\rho} & 0 & 0 & 1 \end{bmatrix}$$

The details of the numerical scheme are explained in Owis [5], Roe [6] and Chakravarthy [7].

5. IMPLICIT SCHEME

The time derivatives in the governing equations are integrated implicitly with the time as explained by Owis [5], barth [8], and Yee [9], Chakravarthy [10] and Kwak [11].

$$\Gamma_e(\frac{\partial \overline{Q}}{\partial t})^{n+1}+(\frac{\partial \overline{E}}{\partial \xi})^{n+1}+(\frac{\partial \overline{F}}{\partial \eta})^{n+1}+\alpha(\overline{H})^{n+1}=(\frac{\partial \overline{E_v}}{\partial \xi})^{n+1}+(\frac{\partial \overline{F_v}}{\partial \eta})^{n+1}+\alpha(\overline{H_v})^{n+1}$$

Application of a first order backward Euler formula to this system of equations yields the following delta form equation:

$$[\frac{\Gamma_e}{J\Delta t}I+(\frac{\partial R}{\partial \overline{Q}})^n]\Delta\overline{Q}=-R^n$$

Where R is the residual vector.

6. THERMOCHEMISTRY MODEL

A thermochemical module is developed based on the assumption of chemical equilibrium of the dissociation reactions. This module is used to evaluate the equilibrium composition and the temperature of the gases at a given enthalpy and pressure. The flow variables such as the pressure and enthalpy are computed using numerical solution of the Navier-Stokes equations as described in the previous sections. The chemical equilibrium module assumes conservation of elements and chemical equilibrium between the different species.

There are several methods used to determine the equilibrium composition including the method of equilibrium constants and the Gibbs function. In the current study, the method of equilibrium constants is adopted to calculate the chemical composition of the exhaust gases. The system used to determine the equilibrium composition at given pressure and enthalpy is formed by a set of linear equations representing the conservation of the species and by the equations which can be written linearly in logarithmic form and represent the equilibrium between the various species.

Conservation equations can be written for the various elements in the gas mixture such as carbon, hydrogen, oxygen and all other chemical elements in the gases as follows:

$$\sum_i a_i n_i = A_k$$

where i is the number of species in the gases and A_k is the chemical content of element k in the fuel and oxidizer.

For every equilibrium reaction of the following form:

$$a\,A+b\,B \underset{\longleftarrow}{\overset{k_p}{\longrightarrow}} c\,C+d\,D$$

There is an equation for the equilibrium constant k_p

$$k_p=\frac{[C]^c[D]^d}{[A]^a[B]^b}(p)^{c+d-a-b}$$

Where p is the pressure and [C] is the concentration of specie [C] = n_c/n_t

Such a system can be solved by trial and error. It can be linearized by choosing arbitrary values for the numbers of moles n_i^o .if ξ_i^o is sufficiently small, then by writing:

$$n_i=n_i^o(1+\xi_i^o)$$

We obtain: $\ln(n_i)\approx\ln(n_i^o)+\xi_i^o$

This system is linear with respect to ξ_i^o and can be solved by the standard methods. The value of ξ_i^o obtained from this system provides new values for the species number of moles as follows,

$$n_i^1=n_i^o(1+\xi_i^o)$$

The convergence of the system is given by the expression:

$$c=\left|A_1-A_1^o\right|+|.....|+\left|\ln(\frac{a_1}{a_1^o})\right|+|.....|$$

And the system is solved when c becomes sufficiently small.

Then at certain pressure and enthalpy computed from the solution of Navier-Stokes equations, we can calculate the temperature using the following equation of state:

$$H=\sum_{i=1}^{n}n_i(Q_f+\int_{Ts}^{T}c_{p_i}dT)$$

Where H is the enthalpy, n_i is the number of moles of species i, Q_f is the heat of formation, c_{p_i} is specific heat at constant pressure of species i, and T_s is standard temperature. The specific heat of the mixture Cp_m and gas properties are calculated for the equilibrium flow as follows:

$$C_{p_m}=C_{p_f}+C_{p_r}$$

Where

$$Cpf = \sum_{i=1}^{N} n_i c_{p_i} / n_t$$

$$C_{p_r} = \sum (n_i / n_t) \frac{H_i (D_T)_i}{T}$$

$$H_i = (Q_f)_i + \int_{Ts}^{T} (C_p)_i dT$$

$$M_w = \sum \frac{n_i}{n_t} M_i$$

$$R_m = Ru / M_w$$

$$\gamma_s = \frac{C_{p_m}}{C_{p_m}(1-D_p) - n_t Ru (1+D_T)^2}$$

$$D_p = (\frac{\partial \ln n_t}{\partial \ln p})_T \qquad and \qquad D_T = (\frac{\partial \ln n_t}{\partial \ln T})_p$$

Where C_{pf} is specific heat for frozen flow, C_{pr} is the contribution of the chemical reaction at equilibrium, *Ru* is the universal gas constant, *Mw* is the molecular weight of the mixture and D_p, D_T are coefficients which express the variation in composition around a mean value.

7. BOUNDARY CONDITIONS

Different boundary conditions are used in the simulations, including inflow, outflow, symmetry and no-slip boundary conditions. All of the boundary conditions are treated implicitly in the code to reduce the restriction on the time step and to increase the stability of the code.

8. RESULTS

8.1. Transonic and non-reactive nozzle flow

An axisymmetric convergent-divergent axisymmetric nozzle with a subsonic inlet and supersonic outlet is simulated numerically. The fluid is assumed to be air and nozzle flow is computed in this case with no chemical reactions. The current results of this non reactive nozzle flow are compared with the same case presented by Eggers [12]. In the simulation of this case, Reynolds number is computed based on the inlet flow conditions and the exit diameter as follows,

$$R_e = \frac{\gamma P_i M_i D_e}{a_i \mu_i}$$

Where a_i the speed of sound at the inlet, $\gamma = 1.4$, $\mu_i = 1.84X10^{-5}, D_e = 0.3021m.$

The Mach number and the static pressure at the inlet are assumed to be M_i=0.14, P_i=11.03 bar, respectively. Therefore, Reynolds number is taken to be R_e=10.37x10^6. The nozzle back pressure (P_{back}) is assumed to be 1.0 bar and T_i=292 K. The inlet conditions of the nozzle and the back pressure are selected such that this test case is shock free. The contours of the non-dimensional static pressure, Mach number and static temperature are introduced in Figure-1, Figure-2 and Figure-3. The axial velocity profile at the nozzle exit is compared with that obtained by Eggers [12] as shown in Figure-4 and the results are in good agreement. Similar observation is obtained by comparing the axial velocity-density profile with the profile of Eggers [12] as clear from Figure-5. Good agreement is observed except near the wall due to different turbulence model adopted by Eggers [12] which is Spalart-Allmaras turbulence model.

Grid sensitivity analysis is introduced in Figure-7 where the variation of the nozzle Mach number at the centerline is computed at two different grid sizes. The results indicate that for the coarse grid of size 150x50, a value of 2.15 Mach number is obtained at the exit. This result is less than that computed by Eggers which is 2.25 while for a fine grid of size 180x50; an exit Mach number of 2.21 is obtained. Therefore, the grid size of 180x50 is considered to be enough for accurate simulation. The simulations of this non-reactive and shock free nozzle flow are performed for different accuracies of the upwind scheme as shown in Figure-6. Comparison of the Mach number along the centerline for first order and third order upwind flux difference scheme indicates that oscillation at the exit is observed for third order upwind flux difference scheme due to lack of enough dissipation. Therefore, first order upwind flux difference scheme is adopted in the current study.

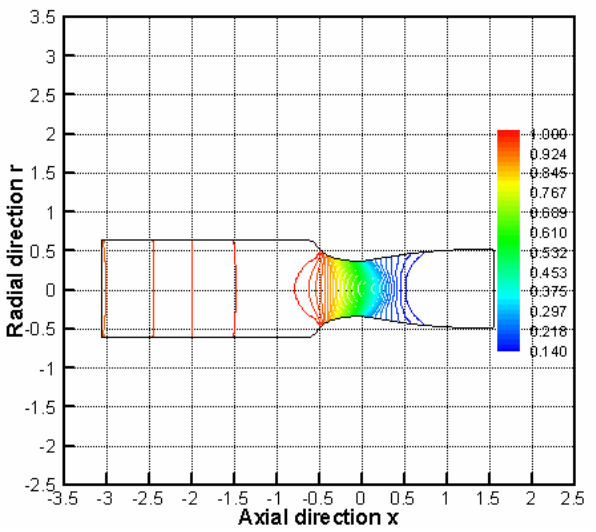

Figure-1. Contours of the non-dimensional static pressure (P/Pi) in the nozzle.

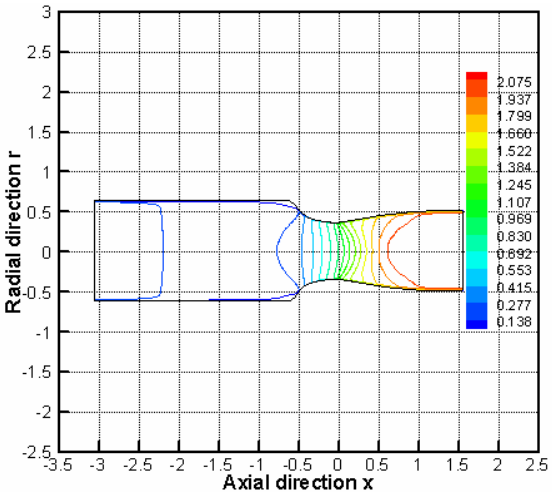

Figure-2. Mach number contours.

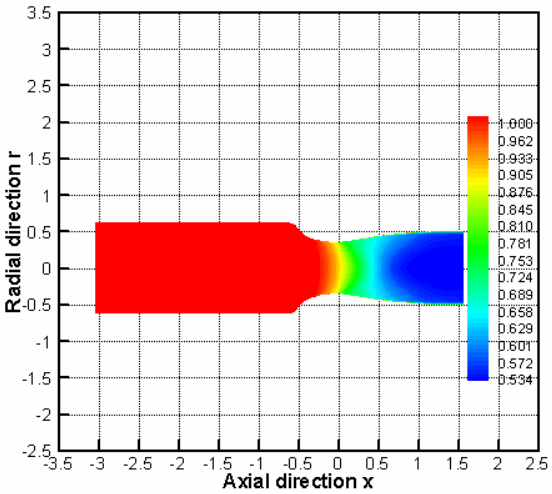

Figure-3. Contours of the static temperature (T/T_i).

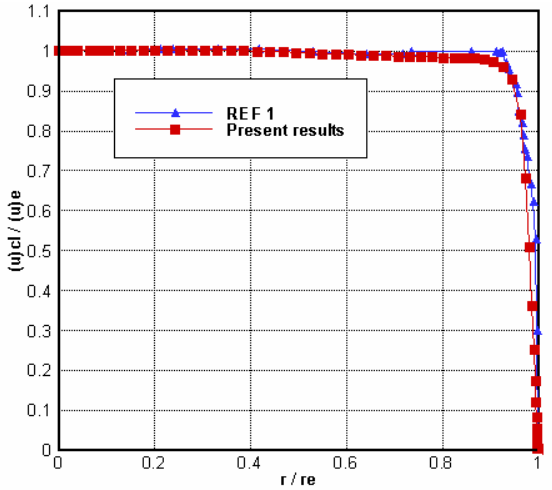

Figure-4. Centerline axial velocity referenced to exit velocity comparison with REF [12].

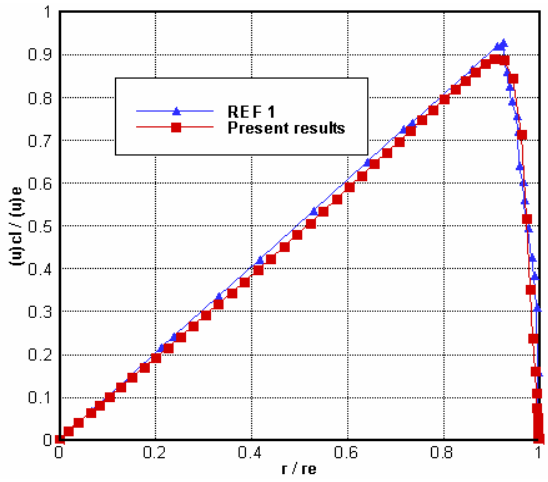

Figure-5. (Density x axial velocity) at centerline referenced to exit (density x axial velocity) comparison with REF [12].

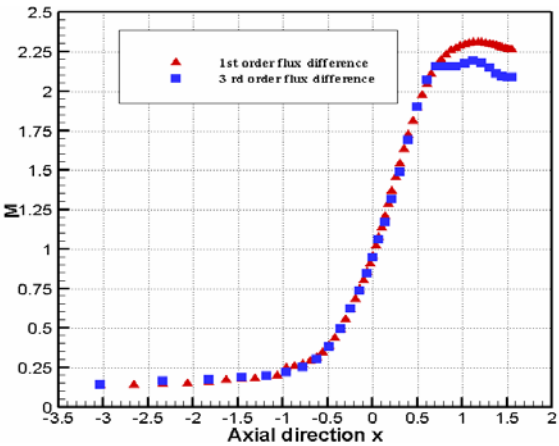

Figure-6. Variation of Mach number along the centerline, with 180 x 50 grid points.

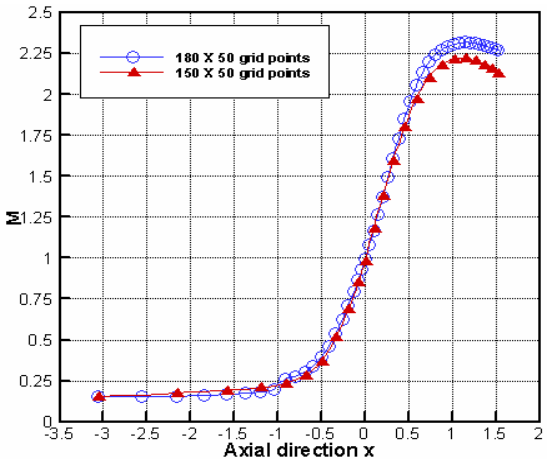

Figure-7. Variation of Mach number along the centerline, with first order upwind flux difference scheme and two grid sizes.

8.2. Reactive flow space shuttle main engine nozzle

The flow in the nozzle of the space shuttle main engine with chemical reactions is simulated numerically. The geometry of this case and the grid used in the simulations are shown in Figure-8. A grid size of 51x51 I used in the simulations. This test case is also solved by Cinnella [1] using chemical equilibrium. The inlet conditions at the nozzle are assumed to be Mach number M_i=0.5, static pressure P_i=202.4 bar, static temperature T_i=3639 K, and oxygen/hydrogen ratio of 6.0 (fuel rich). The contours of the Mach number for the chemical equilibrium are presented in Figure-9 where a smooth variation of the Mach number in the axial direction is obtained without shock waves. The variation of the Mach number along the nozzle centerline with two different assumptions for the chemical reactions is introduced in Figure-10. The chemical equilibrium assumption yields lower exit Mach number than the frozen flow. The chemical equilibrium assumption produces greater thrust force than the frozen flow.

The non-dimensional static temperature contours of the chemical equilibrium flow are presented in Figure-11. The results indicate that static temperature at the nozzle exit is decreased to 0.3 of the nozzle inlet static temperature for the chemical equilibrium while lower exit temperature is obtained with the frozen flow assumption as clear from Figure-12. The chemical equilibrium assumption yields accurate results for the nozzle simulations than the frozen flow. Contours of the static pressure are introduced in Figure-13 where smooth variation of the static pressure along the nozzle is obtained and no shock waves exist in the flow.

The chemical composition of the exhaust gases is computed using the chemical equilibrium assumption and the results are compared with those obtained by Cinnella [1] for the same case as indicated in Figure-14 through Figure-19. The numerical results obtained in the current study are in good agreement with the results computed by Cinnella [1]. The results indicate that the concentration of the hydrogen (H_2) in the exhaust gases is very high because the propellant is fuel rich. The concentration of the hydrogen in the gases is about 80%. The dissociation of the chemical species is reduced as the flow expands in the nozzle and the temperature is reduced. Therefore, no dissociation is observed after x=2.0 in the divergent part of the nozzle as shown in the Figures 16, 17, 18 and 19.

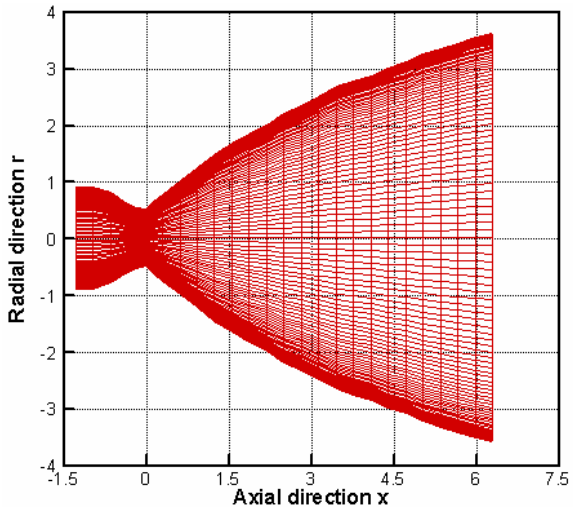

Figure-8. 51x51 Grid points for SSME nozzle.

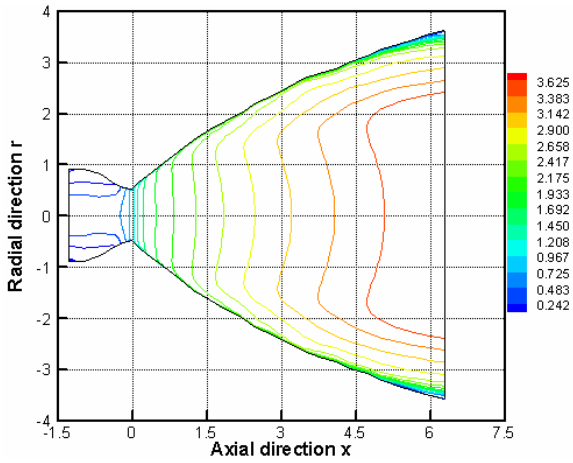

Figure-9. Mach number distribution for SSME.

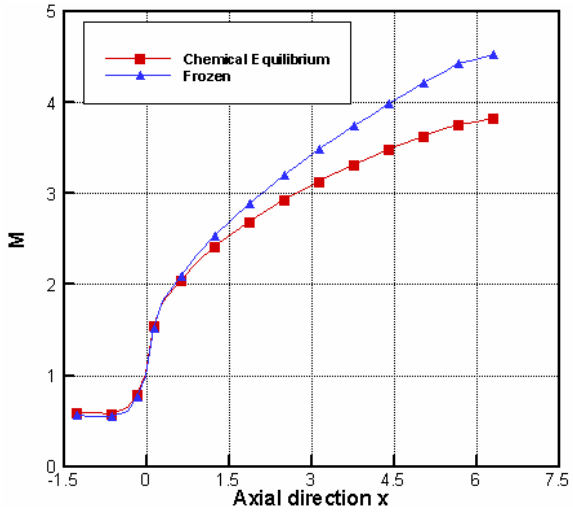

Figure-10. Comparison of the centerline Mach number computed using frozen flow and chemical equilibrium flow.

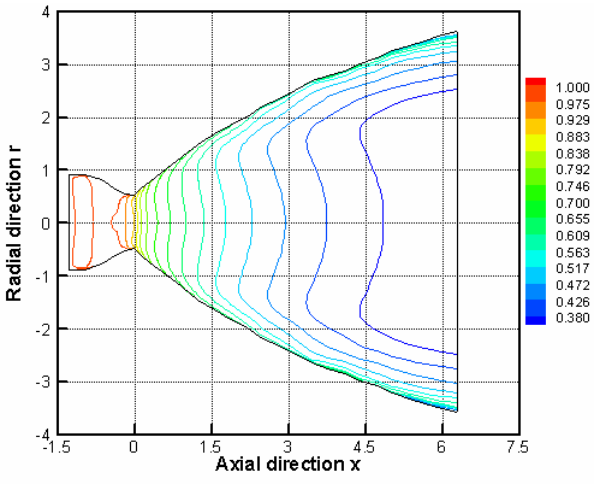

Figure-11. Static temperature (T/Ti) distribution.

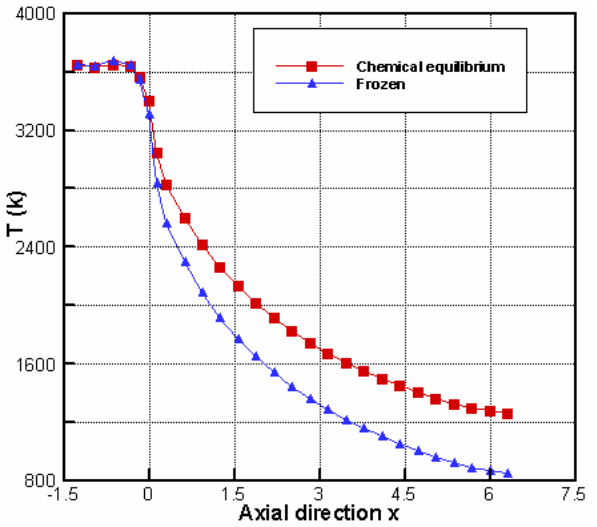

Figure-12. Comparison of equilibrium and frozen flow temperature along centerline.

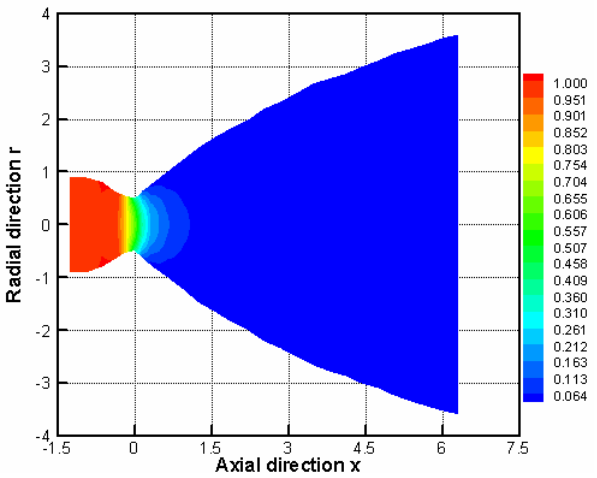

Figure-13. Static pressure (P/Pi) distribution.

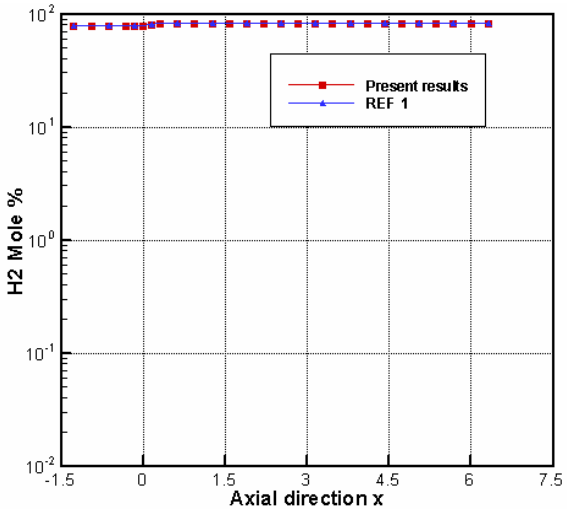

Figure-14. H_2 Mole fraction comparison with REF 1.

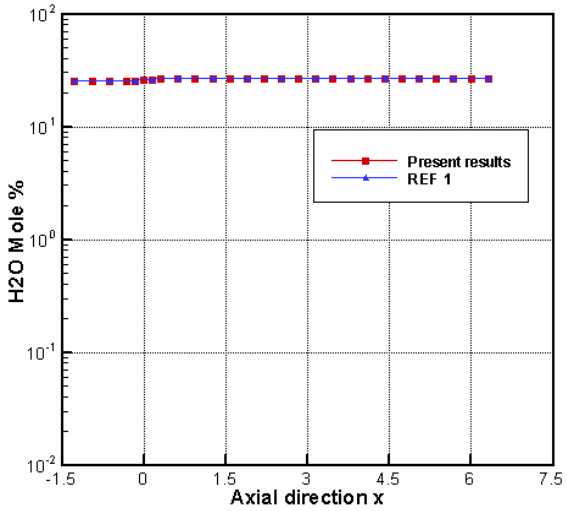

Figure-15. H_2O Mole fraction comparison with REF 1.

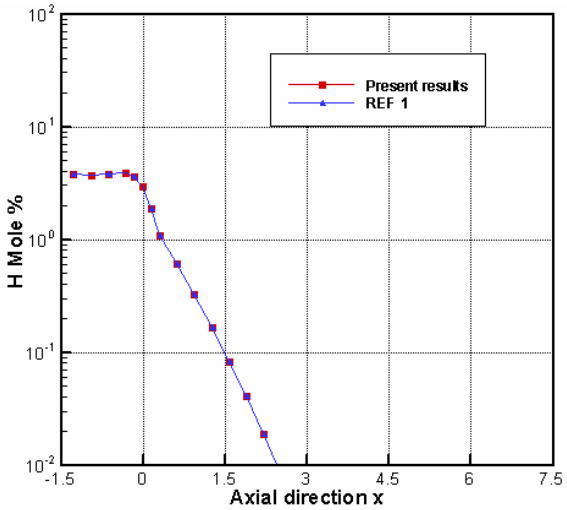

Figure-16. H Mole fraction comparison with REF 1.

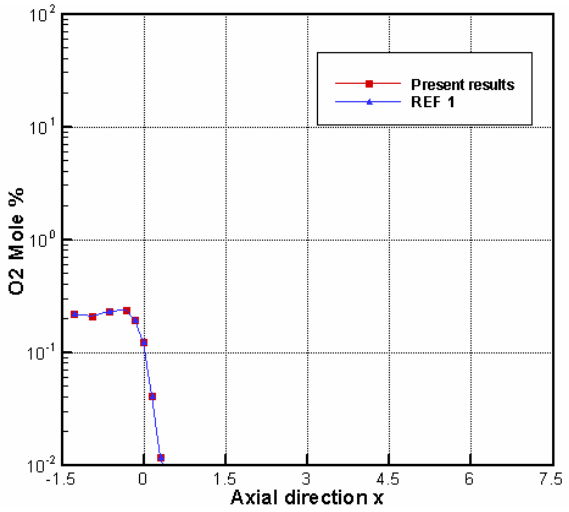

Figure-17. O_2 Mole fraction comparison with REF 1.

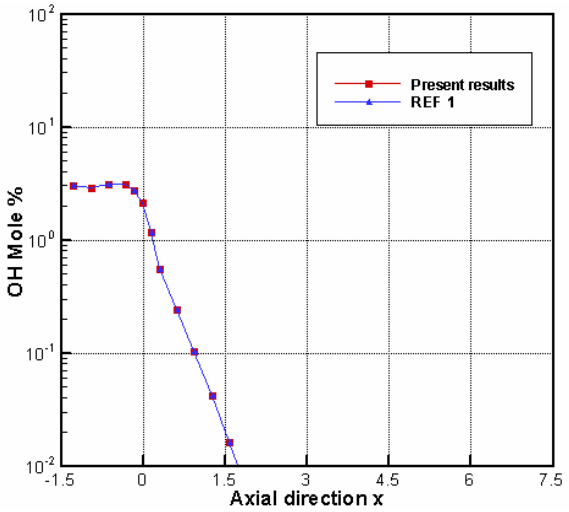

Figure-18. OH Mole fraction comparison with REF 1.

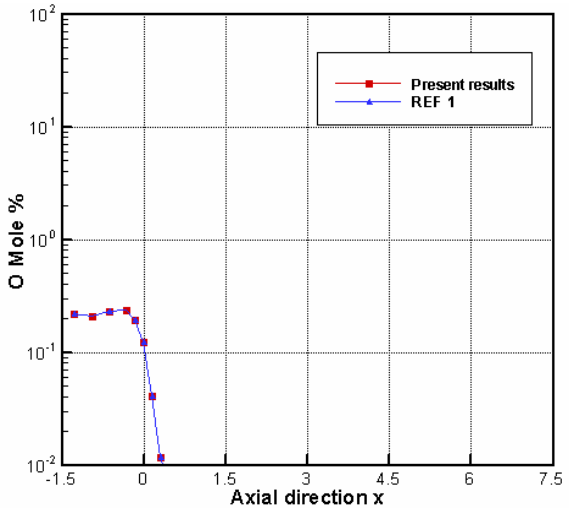

Figure-19. O Mole fraction comparison with REF 1.

9. CONCLUSIONS

A two-dimensional compressible Navier-Stokes solver is developed to simulate reactive flow with the assumption of chemical equilibrium. The code is used to compute nozzle flows with and without reactive flow. The governing equations are solved numerically on a structured grid using the finite difference technique. Flux difference splitting scheme of first or third order accurate is used for the discretization of the convective terms, while second-order central difference is used for the discretization of the viscous terms. A chemical equilibrium module is developed using the method of equilibrium constants and the module is coupled with flow solver to compute the temperature and the thermodynamic properties of the exhaust gases. The code is validated by comparing the results of non-reactive and reactive nozzle flows with the published data and the current results show excellent agreement with the published simulations.

REFERENCES

[1] Carey F. Cox and Pasquale Cinnella. 1994. General Solution Procedure for Flows in Local Chemical Equilibrium. AIAA Journal. 32: No. 3.

[2] R C Mehta. Numerical simulation of high-speed turbulent reacting coaxial jet flow using a structured grid. Proc Instn. Mech. Engrs. Vol. 214 part G.

[3] W. Shawn Westmoreland and Pasquale Cinnella. 1998. Limitations of a Reduced Model for the Simulation of Hydrogen / Air combustion. American Institute of Aeronautics and Astronautics.

[4] Roe P. L. 1981. Approximate Riemann Solvers, Parameter Vectors, and Difference Schemes. J. Comput. Phys. 43, pp. 357-372.

[5] F. M. Owis and Ali H. Nayfeh. 2003. Computations of the Compressible Multiphase Flow over the Cavitating High-Speed Torpedo. ASME Journal of Fluids Engineering. May, Vol. 125.

[6] Stuart E. Rogers, Florian Menter, Paul A. Durbin and Nagi N. Mansour. A Comparison of Turbulence Models in Computing Multi-Element Airfoil Flows. AIAA Paper 94-0291.

[7] Chakravarthy S. R., Szema K-Y., Goldberg U. C. and Gorski J. J. 1985. 'Application of a New Class of High Accuracy TVD Schemes to the Navier-Stokes Equations. AIAA Paper No. 85-0165.

[8] Barth T. J. 1987. 'Analysis of Implicit Local Linearization Techniques for Upwind and TVD Algorithms.' AIAA J. pp. 87-0595.

[9] Yee H. C. 1986. Linearized Form of Implicit TVD Schemes for the Multidimensional Euler and Navier-Stockes Equations. Comp. and Math's. 12A: 413-432.

[10] Chakravarthy S. R. 1985. Relaxation Methods for Unfactored Implicit Upwind Schemes. AIAA J. pp. 84-0032.

[11] Yoon S. Kwak. 1989 .LU-SGS Implicit Algorithm for Three-Dimensional Incompressible Navier-Stokes Equations with Source Term. AIAA J. pp. 89-1964-CP.

[12] Eggers J.M. 1966. Velocity Profiles and Eddy Viscosity Distributions Downstream of a Mach 2.25 Nozzle Exhausting to Quiescent Air. NASA TN D-3601.